PHYSICAL REVIEW A VOLUME 24, NUMBER 4 OCTOBER 1981

Theory of time-delayed measurement: Subnatural linewidth and transient dip spectroscopy

Hai-Woong Lee
Institute for Modern Optics, Department of Physics and Astronomy, University of New Mexico, Albuquerque, New Mexico 87131

Pierre Meystre
Max-Planck Institut für Quantenoptik, D-8046 Garching bei München, West Germany

Marlan O. Scully
Institute for Modern Optics, Department of Physics and Astronomy, University of New Mexico, Albuquerque, New Mexico 87131 and Max-Planck Institut für Quantenoptik, D-8046 Garching bei München, West Germany

(Received 27 April 1981)

Time-delayed measurement of naturally broadened transitions can lead to a narrowing of the linewidth. Moreover, under appropriate conditions, it may result in the appearance of a dip at the line center. An analysis of time-delayed measurement thus provides a theoretical basis for useful optical techniques yielding high spectral resolution. Such an analysis is presented in this work.

I. INTRODUCTION

It has traditionally been one of the main endeavors of spectroscopists to develop measurement techniques yielding ever-higher resolution. In optical experiments the precision of the measurement is often limited by the broadening of the linewidth caused by the interaction of the system under investigation with its environment, such as Doppler effect, collisions, and spontaneous decay. It might seem that, after the Doppler- or collision-broadened width has been eliminated using one of the many schemes introduced in the past for that purpose,[1] the natural linewidth remains the ultimate limit to high-resolution spectroscopy.

Recently, we[2] have proposed and analyzed some spectroscopic techniques which provide resolution beyond the natural linewidth. These considerations are based on the fact[3] that, in the transient regime, the probability for induced transitions in a two-level system interacting with a monochromatic electromagnetic field is not weighted by a Lorentzian of width $\gamma_{ab} \equiv \gamma_a + \gamma_b$, but rather $\delta_{ab} \equiv \gamma_a - \gamma_b$. [$\gamma_a$ and γ_b are the decay rates of the two levels. Note that in this paper, we call γ_a and γ_b the amplitude (rather than population) decay rates. Thus γ_a and γ_b are twice as large as in the usual notation.] As a specific example to demonstrate such transient line narrowing, we have proposed an experimental setup, inspired from delayed detection level-crossing spectroscopy, that utilizes a time delay between the system preparation and the observation of emitted radiation.

Knight and Coleman[4] have shown that a similar result may be achieved in a system of two-level atoms weakly driven by an exponentially decaying laser pulse. In this system, although the lower level is stable, the exponential decay of the pulse amplitude has the same effect on the fluorescence spectrum as would the exponential decay of the lower level. Metcalf and Phillips[5] have shown that despite the loss of signal associated with time-delayed detection, it may still prove very useful in a number of applications. For example, as emphasized in Ref. 2, this technique would allow us to measure the difference $(\gamma_a - \gamma_b)$ directly, and therefore to a much higher precision than could be obtained from independent measurements of γ_a and γ_b.

We note that transient line-narrowing spectroscopy has a number of similarities with detection schemes developed earlier to achieve resolution beyond the natural linewidth in Mössbauer,[6,7] level-crossing,[8–11] and Lamb-shift[12–14] experiments. The common feature of these experiments is to discard the part of the radiation emitted shortly after the preparation of the system and to collect only the delayed and exponentially weakened signal.

In this paper we present a fully quantum-mechanical treatment of time-delayed spectroscopy, both for weak and strong incident fields. In the

discussion of Ref. 2 the atoms were assumed to be driven by a weak classical field, so that a perturbative treatment can be used. In general, the strong-field dynamics is substantially different from the weak-field one. Since the time-delayed spectrum depends sensitively on the temporal behavior of the system, one might expect that the inclusion of power broadening would lead to a different time-delayed spectrum. In fact, as is shown in the second part of this paper, it can lead to the appearance of a transient dip at line center. This dip at line center may prove to be a useful technique to determine accurately the position of the transition. Thus, time-delayed fluorescence measurements have the capability of providing high spectral resolution, not only through the line-narrowing effect, but possibly via strong-field "transient dip spectroscopy".

The goals of the present paper is threefold. First, we show that the results previously obtained semiclassically are recovered exactly in a fully quantum-mechanical treatment. Second, we extend the previous "weak-field" calculations to arbitrary strength driving fields. Third, we give an intuitive physical picture of transient line narrowing and transient dip spectroscopy, based on a well-known feature of the Rabi problem.

The remainder of this paper is organized in the following way: In Sec. II, we give a fully quantum-mechanical theory of transient line narrowing, considering an atom weakly driven by either cw or pulsed excitation. In the case of pulsed excitation, square pulses, as well as exponentially decreasing pulses, are considered. We show that this leads to exactly the same results as the semiclassical theory,[2,4] provided spontaneous emission directly between the two states under consideration is neglected, and the emitted photons from the two states are distinguishable. In Sec. III the effect of power broadening on the time-delayed spectrum is studied. It is shown that the inclusion of power broadening leads to the appearance of a transient dip. Finally, Sec. IV is a summary and discussion. Throughout the paper, natural units $\hbar=c=1$ are used, unless otherwise stated.

II. QUANTUM-MECHANICAL THEORY OF TRANSIENT LINE NARROWING: WEAK-FIELD LIMIT

A. Four-level atom driven by weak cw radiation

We first consider the system previously investigated by Meystre, Scully, and Walther.[2] This system consists of an atom with two unstable levels a and b and a weak cw field driving the atom from the lower level b to the upper level a. If one includes the lower levels to which a and b decay, this may be considered as a four-level atom (see Fig. 1). We prepare the atom in level b and, as the field drives the atom to level a, we count the photons emitted following the $a\rightarrow c$ transition, starting a finite time θ after the atom is prepared. The counting rate is measured as a function of the detuning between the laser frequency k_0 and the energy separation Δ_{ab} between a and b.

Under the rotating-wave approximation and in the interaction picture, the wave function may be written as

$$|\psi(t)\rangle=\alpha^a(t)\,|a,(N-1)\vec{k}_0\rangle+\alpha^b(t)\,|b,N\vec{k}_0\rangle + \int d\vec{k}_1\alpha^c_{\vec{k}_1}(t)\,|c,(N-1)\vec{k}_0,\vec{k}_1\rangle + \int d\vec{k}_2\alpha^d_{\vec{k}_2}(t)\,|d,N\vec{k}_0,\vec{k}_2\rangle\ , \quad (2.1)$$

with

$$|\psi(0)\rangle=|b,N\vec{k}_0\rangle\ . \quad (2.2)$$

Here N is the number of photons in the driving field, $|a,(N-1)\vec{k}_0\rangle$ denotes the state in which the atom is in the state a and $(N-1)$ photons of mode $\vec{k}_0$ are present in the radiation field (and similarly for other eigenstates), and $\vec{k}_0$ is the wave vector of the driving field, $\vec{k}_1$ and $\vec{k}_2$ denote the modes of the photons emitted following the $a\rightarrow c$ and $b\rightarrow d$ transitions, respectively. In writing Eq. (2.1) we have assumed that the energy separations between any two levels are sufficiently different from one another that the photons $\vec{k}_0$, $\vec{k}_1$, and $\vec{k}_2$ are distinguishable. We also have assumed that spontaneous emission from a to b can be neglected. Substituting Eq. (2.1) into the Schrödinger equation, we im-

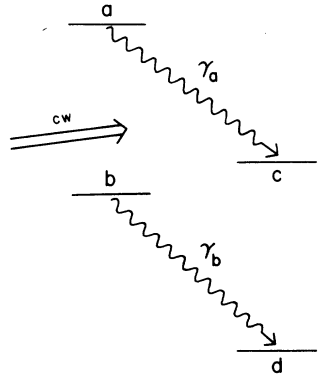

FIG. 1. Four-level atom driven by cw radiation.

mediately obtain the following equations for the probability amplitudes

$$i\frac{d}{dt}\alpha^a(t)=\sqrt{N}M^*_{\vec{k}_0}\exp[i(\Delta_{ab}-k_0)t]\alpha^b(t)+\int d\vec{k}_1 M^*_{\vec{k}_1}\exp[i(\Delta_{ac}-k_1)t]\alpha^c_{\vec{k}_1}(t)\ , \tag{2.3a}$$

$$i\frac{d}{dt}\alpha^b(t)=\sqrt{N}M_{\vec{k}_0}\exp[-i(\Delta_{ab}-k_0)t]\alpha^a(t)+\int d\vec{k}_2 M^*_{\vec{k}_2}\exp[i(\Delta_{bd}-k_2)t]\alpha^d_{\vec{k}_2}(t)\ , \tag{2.3b}$$

$$i\frac{d}{dt}\alpha^c_{\vec{k}_1}(t)=M_{\vec{k}_1}\exp[-i(\Delta_{ac}-k_1)t]\alpha^a(t)\ , \tag{2.3c}$$

$$i\frac{d}{dt}\alpha^d_{\vec{k}_2}(t)=M_{\vec{k}_2}\exp[-i(\Delta_{bd}-k_2)t]\alpha^b(t)\ , \tag{2.3d}$$

subject to the initial condition, Eq. (2.2), or

$$\alpha^b(0)=1\ , \tag{2.4a}$$

$$\alpha^a(0)=\alpha^c_{\vec{k}_1}(0)=\alpha^d_{\vec{k}_2}(0)=0\ . \tag{2.4b}$$

Δ_{ij} is the energy separation between the states i and j, k_i is the energy of a photon, i.e., $k_i=|\vec{k}_i|$, and $M_{\vec{k}}$ is the atomic-transition amplitude defined as

$$\langle j,\vec{k}\,|H_I|\,i,0\rangle=M_{\vec{k}}\exp[-i(\Delta_{ij}-k)t]\ , \tag{2.5}$$

where $i=a$ or b and $j=c$ or d for the present case. H_I denotes the interaction Hamiltonian in the interaction picture.

In order to have an unambiguous definition of the time-delayed power spectrum, one needs to introduce a model detector into the problem.[15] In this paper, we consider the same scheme as in Ref. 2, i.e., we detect the total number of photons spontaneously emitted following the transition $a\rightarrow c$ as a function of the detuning Δ between the driving field and the atomic energy separation $\Delta_{ab}(\Delta\equiv k_0-\Delta_{ab})$. We then define the time-delayed spectrum $N(\Delta,\theta)$ as

$$N(\Delta,\theta)=2\gamma_a\int_\theta^\infty dt_1\,|\,\alpha^a(t_1)\,|^2\ , \tag{2.6a}$$

i.e., as the number of photocounts from time θ on. This can be reexpressed as the number of emitted photons at $t=\infty$ minus that at $t=\theta$,

$$N(\Delta,\theta)=\int d\vec{k}_1\,|\,\alpha^c_{\vec{k}_1}(t=\infty)\,|^2-\int d\vec{k}_1\,|\,\alpha^c_{\vec{k}_1}(t=\theta)\,|^2\ . \tag{2.6b}$$

Thus, the time-delayed photocounts can be obtained by solving Eqs. (2.3) and substituting the solutions into Eqs. (2.6a) or (2.6b). Details of the calculation are shown in Appendix A for the weak-field limit. Here we only show the result

$$N(\Delta,\theta)=\frac{2N\,|\,M_{\vec{k}_0}\,|^2\gamma_a}{\Delta^2+\delta_{ab}^2}\left[\frac{\exp(-2\gamma_a\theta)}{2\gamma_a}+\frac{\exp(-2\gamma_b\theta)}{2\gamma_b}+\frac{2\exp(-\gamma_{ab}\theta)}{\Delta^2+\gamma_{ab}^2}(\Delta\sin\Delta\theta-\gamma_{ab}\cos\Delta\theta)\right]\ , \tag{2.7}$$

where $\delta_{ab}=\gamma_a-\gamma_b$, $\gamma_{ab}=\gamma_a+\gamma_b$, and γ_a and γ_b are the decay rates of levels a and b, respectively.

We note that in the limit $\theta\rightarrow 0$, Eq. (2.7) yields the usual Lorentzian of width γ_{ab}. However, if θ is sufficiently large, only the first or the second term in the large parentheses of Eq. (2.7) remains, depending upon which of γ_a and γ_b is largest. Thus, the dependence of $N(\Delta,\theta)$ on Δ is determined mainly by the Lorentzian prefactor, and the linewidth approaches the difference δ_{ab}. This is the transient line-narrowing effect. In fact, Eq. (2.7) is identical with the expression obtained earlier[2] using the density-matrix equations and a classical description of the field. Here, Eq. (2.7) is obtained using a fully quantum-mechanical approach. The normalized power spectrum $N(\Delta,\theta)$ is shown in Fig. 2 for $\gamma_a=3$ and $\gamma_b=1$, and in Fig. 3 for $\gamma_a=1.01$ and $\gamma_b=1$.

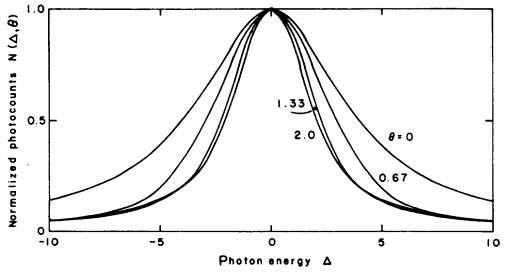

FIG. 2. Normalized photocounts $N(\Delta,\theta)$ as a function of Δ for various values of the delay $\theta=0$, 0.67, 1.33, and 2.0 for the cases $\gamma_a=3$ and $\gamma_b=1$. θ is in units of γ_b^{-1}. If the system under consideration is the one shown in Fig. 1, Δ is the energy detuning between the driving field and the atomic-energy separation. If the system is that shown in Fig. 4, Δ is the energy detuning between the central frequency of the driving pulse and the atomic-energy separation, and γ_b is the decay constant of the exponentially decreasing pulse.

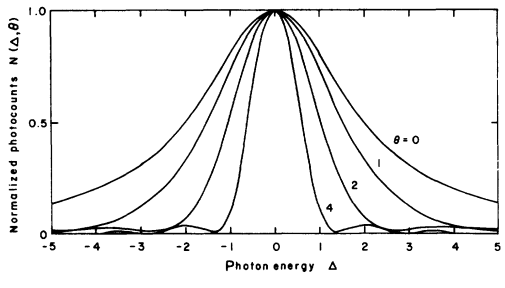

FIG. 3. Same as Fig. 2 except that $\theta=0,1,2,4$ and $\gamma_a=1.01$.

B. Three-level atom driven by weak-pulsed radiation

Knight and Coleman[4] have pointed out that transient line narrowing can also be realized in a system of two-level atoms driven by a weak exponentially decreasing pulse. In fact, the subnatural linewidth observed in Mössbauer experiments[6,7] involves basically the same system. For convenience we introduce, in addition to the two levels a and b, a third level c to which the upper level a can decay (see Fig. 4). Comparison of Figs. 1 and 4 shows the strong analogy between this system and that discussed previously. The only difference is that the exponentially decreasing pumping rate arises now from the exponential decay of the pulse amplitude in Fig. 4 whereas it came from the exponential decay of level b in Fig. 1.

We describe the radiation via its spectral amplitude $\phi(\vec{k})$. For an exponentially decaying pulse, this would be a Lorentzian. However, we keep $\phi(k)$ arbitrary, so that our result is valid for any pulse shape. Let us introduce the operator $B^\dagger$ as[16,17]

$$B^\dagger=\int d\vec{k}\phi(\vec{k})a_k^\dagger , \tag{2.8}$$

where $a_{\vec{k}}^\dagger$ is the usual photon creation operator.

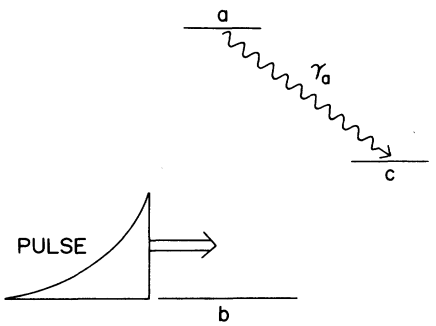

FIG. 4. Three-level atom driven by radiation pulse.

The pulsed radiation can then be represented by

$$|N_\phi\rangle=\frac{1}{\sqrt{N!}}(B^\dagger)^N|\text{vacuum}\rangle , \tag{2.9}$$

where N is the number of photons in the pulse. For simplicity, we take $N=1$ and consistently limit ourselves to the weak-field limit.

As before, we write the wave function as

$$|\psi(t)\rangle=\alpha^a(t)|a,0\rangle+\int d\vec{k}\alpha_{\vec{k}}^b(t)|b,\vec{k}\rangle + \int d\vec{k}_1\alpha_{\vec{k}_1}^c(t)|c,\vec{k}_1\rangle , \tag{2.10}$$

with

$$|\psi(0)\rangle=\int d\vec{k}\phi(\vec{k})|b,\vec{k}\rangle=|b,1_\phi\rangle . \tag{2.11}$$

Substituting Eq. (2.10) into the Schrödinger equation, we obtain

$$i\frac{d}{dt}\alpha^a(t)=\int d\vec{k}M_{\vec{k}}^*\exp[i(\Delta_{ab}-k)t]\alpha_{\vec{k}}^b(t) + \int d\vec{k}_1M_{\vec{k}_1}^*\exp[i(\Delta_{ac}-k_1)t]\alpha_{\vec{k}_1}^c(t) , \tag{2.12a}$$

$$i\frac{d}{dt}\alpha_{\vec{k}}^b(t)=M_{\vec{k}}\exp[-i(\Delta_{ab}-k)t]\alpha^a(t) , \tag{2.12b}$$

$$i\frac{d}{dt}\alpha_{\vec{k}_1}^c(t)=M_{\vec{k}_1}\exp[-i(\Delta_{ac}-k_1)t]\alpha^a(t) . \tag{2.12c}$$

where, as before, we have assumed that Δ_{ab} and Δ_{ac} are sufficiently different from each other so that the photons $\vec{k}$ and $\vec{k}_1$ are distinguishable. Equations (2.12) are subject to the initial condition, Eq. (2.11), or

$$\alpha_{\vec{k}}^b(0)=\phi(\vec{k}),\ \alpha^a(0)=\alpha_{\vec{k}_1}^c(0)=0 . \tag{2.13}$$

The number of photons emitted following the $a\rightarrow c$ transition from the time $t=\theta$ on is given by

$$N(\Delta,\theta)=2\gamma_a\int_\theta^\infty dt_1|\alpha^a(t_1)|^2 = \int d\vec{k}_1|\alpha_{\vec{k}_1}^c(t=\infty)|^2-\int d\vec{k}_1|\alpha_{\vec{k}_1}^c(t=\theta)|^2 . \tag{2.14}$$

This can be obtained by solving Eqs. (2.12) and substituting the solution into Eq. (2.14). Details of the calculation are shown in Appendix B, neglecting spontaneous decay from a to b (γ_a is the decay rate of the $a\rightarrow c$ transition). $N(\Delta,\theta)$, of course, depends on the pulse shape because the solutions of Eqs. (2.12) are different for a different choice of $\phi(\vec{k})$.

For the case of an exponentially decaying pulse, $N(\Delta,\theta)$ is again given by Eq. (2.7). Therefore,

Figs. 2 and 3 also give the normalized count $N(\Delta,\theta)$ for the system considered here. We note, however, that k_0 is now to be interpreted as the central frequency of the pulse, $\Delta=k_0-\Delta_{ab}$, and γ_b is the decay constant of the pulse rather than of the atomic level.

For the case of a square pulse of duration t_0, we obtain

$$N(\Delta,\theta)=\begin{cases}\dfrac{2|g_s|^2\gamma_a}{\Delta^2+\gamma_a^2}\left[t_0-\theta-\dfrac{\exp(-2\gamma_a t_0)-\exp(-2\gamma_a\theta)}{2\gamma_a}\right. \\ \qquad\left.+\dfrac{2\exp(-\gamma_a t_0)(\gamma_a\cos\Delta t_0-\Delta\sin\Delta t_0)-2\exp(-\gamma_a\theta)(\gamma_a\cos\Delta\theta-\Delta\sin\Delta\theta)}{\Delta^2+\gamma_a^2}\right] & \text{for } \theta<t_0\ , \quad (2.15a)\\ \dfrac{|g_s|^2\exp(-2\gamma_a\theta)}{\Delta^2+\gamma_a^2}[1+\exp(2\gamma_a t_0)-2\exp(\gamma_a t_0)\cos\Delta t_0] & \text{for } \theta\geq t_0\ . \quad (2.15b)\end{cases}$$

g_s is a constant depending on the pulse parameters, k_0 is again the central frequency of the pulse, and $\Delta=k_0-\Delta_{ab}$. The normalized count $N(\Delta,\theta)$ is shown in Fig. 5 for $t_0=1$ and $\gamma_a=3$, and in Fig. 6 for $t_0=1$ and $\gamma_a=1.01$. $N(\Delta,\theta)$ takes the same form for all θ's exceeding t_0. This is because, for $\theta>t_0$, the situation is analogous to making time-delayed measurement on a two-level system with the levels a and c. We see that the line narrowing does occur with a square pulse although the narrowing is not as dramatic as that associated with an exponentially decreasing pulse.

C. Physical interpretation of transient line narrowing

Since transient line narrowing arises from the behavior of the system in the transient regime, it is natural to study the temporal behavior of the system in order to better understand and interpret the effect. Intuitively, it is not difficult to understand the line-narrowing effect. It is based on the well-known (but perhaps anti-intuitive) fact that the Rabi frequency is larger for larger detunings, and that therefore the excitation and the depletion of the population of the upper level (level a in our system) are slower when excited exactly on resonance. This means that the remaining population after some delay time θ is relatively a large number when excited on resonance, thus leading to the line narrowing. In this section we show quantitatively that the above interpretation is indeed true. Although our discussion here is limited to the case of an atom driven by pulsed radiation, it can equally be applied to the system considered in Sec. II A provided that the appropriate redefinition of k_0, γ_b, etc., is made.

The integrand $|\alpha^a(t)|^2$ in Eq. (2.14) for the photocount is the probability for the atom to be in the upper state a at time t. For the case of an exponentially decreasing pulse, we find using Eq. (B4) of Appendix B,

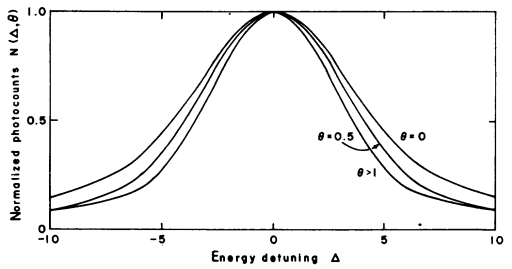

FIG. 5. Normalized photocounts $N(\Delta,\theta)$ as a function of energy detuning for various values of the delay $\theta=0$, 0.5, and $\theta>1$ for the case $\gamma_a=3$. The driving field is assumed to be in the form of a square pulse of duration $t_0=1$. θ is in units of t_0.

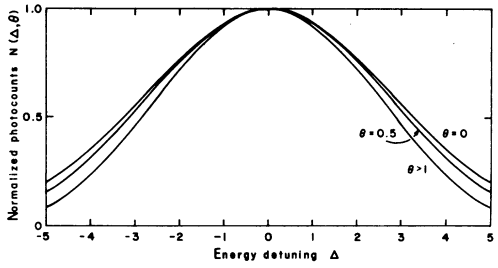

FIG. 6. Same as Fig. 5 except that $\gamma_a=1.01$.

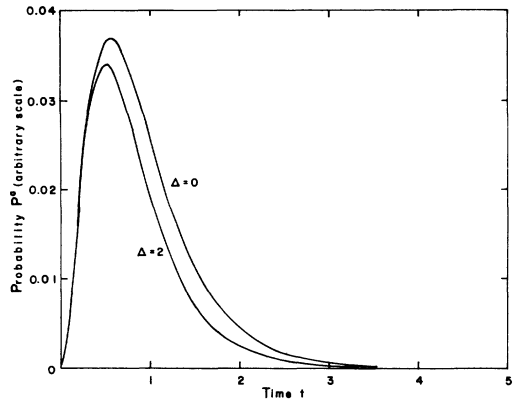

FIG. 7. Probability $P^a(\Delta,t)$ as a function of time t for two values of energy detuning $\Delta=0$ and 2 for the cases $\gamma_a=3$ and $\gamma_b=1$ (exponentially decreasing pulse). The time is in units of γ_b^{-1}.

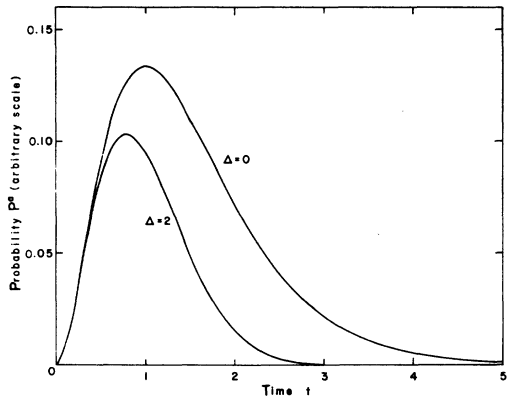

FIG. 8. Same as Fig. 7 except that $\gamma_a=1.01$.

$$p^a(\Delta,t)\equiv|\alpha^a(t)|^2 = \frac{|g_e|^2}{\Delta^2+\delta_{ab}^2}[\exp(-2\gamma_a t)+\exp(-2\gamma_b t) -2\exp(-\gamma_{ab}t)\cos\Delta t]\ . \quad (2.16)$$

$p^a(\Delta,t)$ is plotted in Fig. 7 as a function of time for two different values of detuning $\Delta=0$ and 2 for the case $\gamma_a=3$ and $\gamma_b=1$, and in Fig. 8 for $\gamma_a=1.01$ and $\gamma_b=1$. $p^a(\Delta,t)$ initially increases as the driving field pumps the atom to level a, goes through a peak and eventually decreases to zero because of spontaneous emission. The peak occurs earlier and has a smaller value for $\Delta=2$. This reflects the above-mentioned fact that the Rabi frequency is larger for larger detunings and is the key point in understanding the line-narrowing effect. According to Eq. (2.14), $N(\Delta,\theta)$ is the area under the probability curve between $t=\theta$ and ∞. We see from Fig. 7 that, as θ is increased, this area decreases faster for larger Δ. This is even more clear in Fig. 8. The integral of $p^a(\Delta,t)$ between, for example, $t=2$ and ∞ is only a small fraction of the area between $t=0$ and ∞ for the case $\Delta=2$, while it is still a large fraction for the case $\Delta=0$. Thus, the larger Δ, the faster the system emits spontaneously and leaves a smaller number of photons to be emitted after some delay time θ. This directly leads to the narrowing of the linewidth.

For a square pulse of duration t_0, the probability takes the form

$$p^a(\Delta,t)=\begin{cases} |\alpha^a(t)|^2=\dfrac{|g_s|^2}{\Delta^2+\gamma_a^2}[1+\exp(-2\gamma_a t)-2\exp(-\gamma_a t)\cos\Delta t], \text{ for } t\le t_0 & (2.17a) \\ |\alpha^a(t)|^2=\dfrac{|g_s|^2\exp(-2\gamma_a t)}{\Delta^2+\gamma_a^2}[\exp(2\gamma_a t_0)+1-2\exp(\gamma_a t_0)\cos\Delta t_0], \text{ for } t>t_0 & (2.17b) \end{cases}$$

where Eqs. (B8) of Appendix B have been used. This probability is plotted in Fig. 9 as a function of time for two different values of detuning for the case $t_0=1$, $\gamma_a=1.01$. Here again we see that the peak occurs earlier and has a smaller value for larger detunings, although the effect is not as strong as before. This explains a relatively weak line narrowing with a square pulse.

III. STRONG-SIGNAL REGIME: TRANSIENT DIP SPECTROSCOPY

Up to now, we have restricted ourselves to the weak-field limit, in which the use of a perturbative treatment is justified. We now relax this restriction and study time-delayed spectroscopy in the strong-signal regime.

The analysis departs from that of the weak-field limit in that instead of using Eq. (A5) of Appendix A, we now solve Eqs. (A2) and (A3) exactly for $\alpha^a(t)$ and $\alpha^b(t)$. These equations yield a second-order differential equation for $\alpha^a(t)$ [and also for $\alpha^b(t)$], with the solution[3]

$$\alpha^a(t)=-i\sqrt{N}M^*_{\vec{k}_0}\exp(u_2 t)\int_0^t dt_1\exp[(u_1-u_2)t_1]\,, \tag{3.1}$$

where

$$u_1=\{-\gamma_{ab}-i\Delta+[(\delta_{ab}+i\Delta)^2-4N\,|\,M_{\vec{k}_0}\,|^2]^{1/2}\}/2\,, \tag{3.2a}$$

$$u_2=\{-\gamma_{ab}-i\Delta-[(\delta_{ab}+i\Delta)^2-4N\,|\,M_{\vec{k}_0}\,|^2]^{1/2}\}/2\,. \tag{3.2b}$$

Using Eqs. (3.1) and (2.3c) we get

$$\alpha^c_{\vec{k}_1}(t)=(-i)^2\sqrt{N}M^*_{\vec{k}_0}M_{\vec{k}_1}\int_0^t dt_1\exp[u_2-i(\Delta_{ac}-k_1]t_1\int_0^{t_1}dt_2\exp(u_1-u_2)t_2\,. \tag{3.3}$$

The number of photons emitted during the time interval (θ,∞) following the $a\rightarrow c$ transition is again given by Eq. (2.6a) or (2.6b). After tedious but straightforward algebra, we obtain

$$N(\Delta,\theta)=[4\gamma_a N\,|\,M_{\vec{k}_0}\,|^2\exp(-\gamma_{ab}\theta)]/\rho \times\left[\frac{\gamma_{ab}\cosh[\theta\sqrt{\rho}\cos(\phi/2)]+\sqrt{\rho}\cos(\phi/2)\sinh[\theta\sqrt{\rho}\cos(\phi/2)]}{\gamma_{ab}^2-\rho\cos^2(\phi/2)} -\frac{\gamma_{ab}\cos[\theta\sqrt{\rho}\sin(\phi/2)]-\sqrt{\rho}\sin(\phi/2)\sin[\theta\sqrt{\rho}\sin(\phi/2)]}{\gamma_{ab}^2+\rho\sin^2(\phi/2)}\right], \tag{3.4}$$

where

$$\rho=[(\delta_{ab}^2-\Delta^2-4N\,|\,M_{\vec{k}_0}\,|^2)^2+4\delta_{ab}^2\Delta^2]^{1/2}\,, \tag{3.5}$$

and ϕ is determined by

$$\cos\phi=(\delta_{ab}^2-\Delta^2-4N\,|\,M_{\vec{k}_0}\,|^2)/\rho\,, \tag{3.6a}$$

$$\sin\phi=2\delta_{ab}\Delta/\rho\,. \tag{3.6b}$$

Equation (3.4) is the main result of this section. The time-delayed count $N(\Delta,\theta)$ is, in general, a complicated function of the system parameters, and we first consider some limiting cases.

A. Weak-field limit

In the weak-field limit $N\rightarrow 0$, we obtain

$$\rho\simeq\delta_{ab}^2+\Delta^2\,, \tag{3.7a}$$

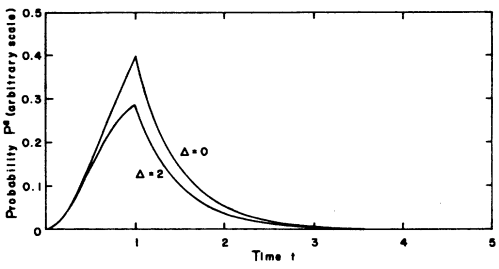

FIG. 9. Probability P^a as a function of time t for two values of energy detuning $\Delta=0$ and 2 for the case $t_0=1$ (square pulse) and $\gamma_a=1.01$. t is in units of t_0.

$$\cos\phi\simeq(\delta_{ab}^2-\Delta^2)/\rho\,, \tag{3.7b}$$

$$\sin\phi\simeq 2\delta_{ab}\Delta/\rho\,. \tag{3.7c}$$

Equation (3.4) reduces then to Eq. (2.7) of Sec. II A, as it should.

B. No time delay

In the limit $\theta\rightarrow 0$ (no time delay), Eq. (3.4) becomes

$$N(\Delta,\theta=0)=\frac{N\,|\,M_{\vec{k}_0}\,|^2\gamma_{ab}}{\gamma_b(\Delta^2+\gamma_{ab}^2+N\,|\,M_{\vec{k}_0}\,|^2\gamma_{ab}^2/\gamma_a\gamma_b)}\,, \tag{3.8}$$

which is the well-known power-broadened Lorentzian line shape.

C. General case

We now return to the general formula Eq. (3.4). In Figs. 10 and 11, $N(\Delta,\theta)$ is plotted as a function of the detuning $\Delta(\equiv k_0-\Delta_{ab})$ for different delay times θ and for different field intensities for the case $\gamma_a=3$ and $\gamma_b=1$. We immediately see a new feature of the power-broadened spectrum, namely, the appearance of a dip at line center for large θ and for high enough field intensities. A close investigation indicates that, for a fixed value of the field intensity, and as θ is increased from zero, the linewidth first decreases (transient line narrowing). However, as θ is further increased, the line broadens back until the linewidth becomes roughly the same as that at $\theta=0$. If θ is further increased beyond this point, a narrow dip appears at line center, and becomes deeper and wider as θ is further increased. Since it always appears at line center, it may help locate the center of a transition with improved accuracy over standard methods. The dip appears with a smaller delay for stronger fields. Thus, one can operate without significant loss of signal. For example, for a Rabi frequency $G(\equiv N\,|M_{\vec{k}_0}|^2)=1.5$, the dip appears already at $\theta=2$. On the other hand, for $G=0.6$, the dip still does not appear even for θ as large as 4. In Fig. 12 we show $N(\Delta,\theta)$ at a fixed θ as G is varied. Here again, we see clearly that the dip appears more easily for stronger fields.

In Fig. 13 we show the same $N(\Delta,\theta)$ versus Δ curve for the cases $\gamma_a=1.01$ and $\gamma_b=1$, and $G=1$ for various θ. We immediately notice the strong oscillatory behavior exhibited in this case.

A useful parameter to determine the behavior of $N(\Delta,\theta)$ is the ratio of the Rabi frequency to δ_{ab}, or

$$r\equiv G^2/\delta_{ab}^2 \ . \tag{3.9}$$

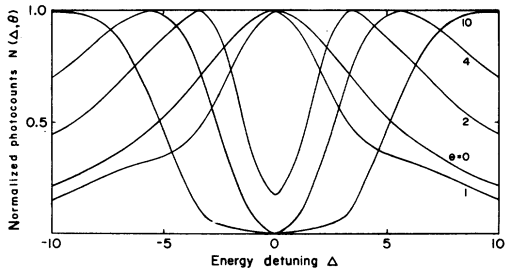

FIG. 11. Same as Fig. 10 except that $\theta=0,1,2,4,10$ and $G=1.5$.

This ratio determines whether the arguments of the hyperbolic functions are larger or smaller than those of the sinusoidal functions in Eq. (3.4), and therefore determines the characteristic behavior of $N(\Delta,\theta)$. For the case of Fig. 13, r is very large ($r=10^4$) and the contribution from the sinusoidal terms is important. As a result $N(\Delta,\theta)$ exhibits a strong oscillatory behavior. On the other hand, r is relatively small ($r<1$) for the cases shown in Figs. 10 and 11, and no strong oscillatory behavior is exhibited there.

In a sense the transient dip is an opposite phenomenon to the line narrowing because, in order for the dip to appear, the remaining population of the upper level a after the delay time θ should be a relatively small number when excited on resonance. That is, the depletion of the population of level a should be faster when excited on resonance. That this is indeed the case when θ is sufficiently large can be seen in Fig. 14, where the probability $p^a(\Delta,t)\equiv|\alpha^a(t)|^2$ for the atoms to be in level a is plotted as a function of time for two different values of detuning for the cases $\gamma_a=3$, $\gamma_b=1$, and $G=0.6$. As we have already noted in the previous section, the peak occurs earlier and has a smaller

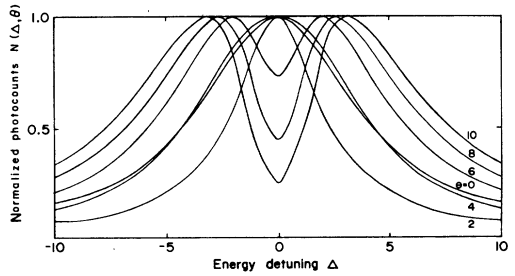

FIG. 10. Normalized photocounts $N(\Delta,\theta)$ as a function of energy detuning Δ for various values of the delay $\theta=0,2,4,6,8,10$ for the case $\gamma_a=3$, $\gamma_b=1$, and the Rabi frequency $G=N\,|M_{\vec{k}_0}|^2=0.6$. θ is in units of γ_b^{-1}.

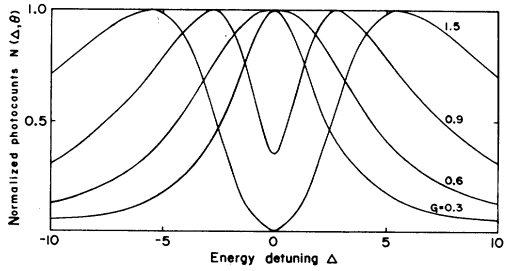

FIG. 12. Normalized photocounts $N(\Delta,\theta)$ as a function of energy detuning Δ for various values of the field intensity $G=0.3$, 0.6, 0.9, and 1.5 for the cases $\gamma_a=3$, $\gamma_b=1$, and for a fixed delay time $\theta=4$. θ is in units of γ_b^{-1}.

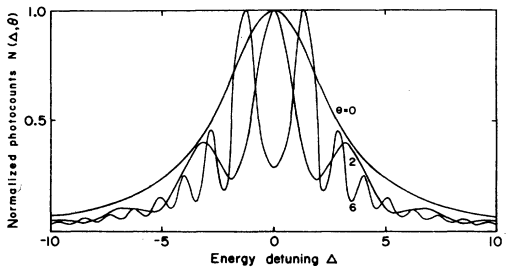

FIG. 13. Normalized photocounts $N(\Delta,\theta)$ as a function of energy detuning Δ for various values of the delay $\theta=0,2,6$ for the cases $\gamma_a=1.01$, $\gamma_b=1$, and $G=1$. θ is in units of γ_b^{-1}.

value for $\Delta=2$. This of course accounts for the narrowing of the linewidth for small values of the delay time θ. However, when θ is sufficiently large, the $\Delta=2$ curve finally catches up with the $\Delta=0$ curve. This behavior can be understood if we note that for a large detuning the atom is inefficiently pumped to level a and therefore still a large number of atoms are available to be pumped at a large time. This means a slower depletion of level a at sufficiently large time when excited off resonance and leads directly to the appearance of a dip at line center.

IV. SUMMARY AND DISCUSSION

Under appropriate conditions, time-delayed observation of the radiation emitted during an atomic transition can lead to the narrowing of the linewidth or the appearance of a dip at line center. The linewidth is limited in the small-signal regime by the difference in the transition rates involved. This provides an optical technique that yields high spectral resolution.

A dip may appear at line center as a result of the transient behavior of a system subject to power broadening. Unlike the line-narrowing effect, the width of the dip is not limited by $(\gamma_a-\gamma_b)$, and/or the delay θ. It can be as small as one likes if the intensity of the driving field is close to the threshold for its appearance. This dip suggests a means of enhancing resolution involving homogeneously broadened systems while the Lamb dip is available to study inhomogeneously broadened systems.

The narrowing of the linewidth or the appearance of the dip is achieved at the expense of some loss of the signal. A recent analysis[5] indicates that, despite the signal loss, time-resolved line narrowing is highly desirable in a large number of cases. If one tries to locate line center in the absence of spectral complications, i.e., if we know we have only one line in the region of interest, then it may be best to let the delay time $\theta\to 0$ and collect the maximum number of counts, since the determination of the line center improves as the square root of the intensity of the signal. However, if there are complicating circumstances, such as overlapping lines, etc., it may be better to use finite delay times with the attendant line narrowing and/or dip.

We finally note that the results obtained here via a fully quantum-mechanical theory take exactly the same form as those previously derived semiclassically. The origin of this exact agreement lies in the neglect of spontaneous decay from level $|a\rangle$ to $|b\rangle$.

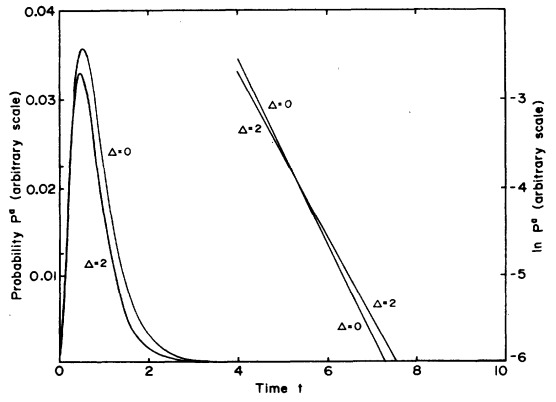

FIG. 14. Probability P^a as a function of time t for two values of energy detuning $\Delta=0$ and 2, for the case $\gamma_a=3$, $\gamma_b=1$, and $G=0.6$. t is in units of γ_b^{-1}. For $t\geq 4$, $\ln P^a$ is plotted as a function of time t and the corresponding scale is shown on the right side of the graph.

ACKNOWLEDGMENT

This research was supported in part by the Air Force Office of Scientific Research, United States Air Force, under Grant No. AFOSR-80-0278.

APPENDIX A: DERIVATION OF EQ. (2.7). THE CASE OF cw RADIATION

In order to derive Eq. (2.7), we first solve Eqs. (2.3). From Eq. (2.3c) we have

$$\alpha^c_{\vec{k}_1}(t)=-iM_{\vec{k}_1}\int_0^t dt_1\exp[-i(\Delta_{ac}-k_1)t_1]\alpha^a(t_1)\ . \tag{A1}$$

Substituting Eq. (A1) into Eq. (2.3a), we obtain

$$\left[\frac{d}{dt}+\gamma_a\right]\alpha^a(t)=-i\sqrt{N}M^*_{\vec{k}_0}\exp(-i\Delta t)\alpha^b(t)\ . \tag{A2}$$

Similarly, from Eqs. (2.3d) and (2.3b), we obtain

$$\left[\frac{d}{dt}+\gamma_b\right]\alpha^b(t)=-i\sqrt{N}M_{\vec{k}_0}\exp(i\Delta t)\alpha^a(t)\ . \tag{A3}$$

The decay rates γ_a and γ_b in Eqs. (A2) and (A3) are defined as

$$\gamma_a=\left[k^2\pi\int d\Omega_{\hat{k}}\,|M_{\vec{k}}|^2\right]_{k=\Delta_{ac}}\ , \tag{A4}$$

γ_b is given by the same expression except that it is evaluated at $k=\Delta_{bd}$ instead of $k=\Delta_{ac}$.

In the weak-field limit (N small, or Rabi frequency $G<<\gamma_a,\gamma_b$), the right side of Eq. (A3) may be neglected. This means that the major source of depleting level b is not the driving field but spontaneous decay to level d. We then have

$$\alpha^b(t)\cong\exp(-\gamma_b t)\ . \tag{A5}$$

Substituting Eq. (A5) into (A2) we then obtain

$$\alpha^a(t)\cong -i\sqrt{N}M^*_{\vec{k}_0}\exp(-\gamma_a t)\int_0^t dt_1\exp[(-\delta_{ab}-i\Delta)t_1] \tag{A6}$$

and therefore, using Eq. (A1),

$$\alpha^c_{\vec{k}_1}(t)\cong(-i)^2\sqrt{N}M^*_{\vec{k}_0}M_{\vec{k}_1}\int_0^t dt_1\exp[-\gamma_a-i(\Delta_{ac}-k_1)]t_1\int_0^{t_1}dt_2\exp[(-\delta_{ab}-i\Delta)t_2]\ . \tag{A7}$$

Substituting Eq. (A6) into (2.6a), or Eq. (A7) into (2.6b), we immediately obtain Eq. (2.7) for the time-delayed photocounts.

APPENDIX B: DERIVATION OF EQS. (2.7) AND (2.15). THE CASE OF PULSED RADIATION

In order to derive Eqs. (2.7) and (2.15) for the case of pulsed radiation, we first solve Eqs. (2.12). From Eqs. (2.12b) and (2.12c), we have

$$\alpha^b_{\vec{k}}(t)=\phi(\vec{k})-iM_{\vec{k}}\int_0^t dt_1\exp[-i(\Delta_{ab}-k)t_1]\alpha^a(t_1)\ , \tag{B1}$$

$$\alpha^c_{\vec{k}_1}(t)=-iM_{\vec{k}_1}\int_0^t dt_1\exp[-i(\Delta_{ac}-k_1)t_1]\alpha^a(t_1)\ . \tag{B2}$$

Substituting Eqs. (B1) and (B2) into Eq. (2.12a), we obtain

$$\left[\frac{d}{dt}+\gamma_a+\gamma'_a\right]\alpha^a(t)=-i\int d\vec{k}M^*_{\vec{k}}\exp[i(\Delta_{ab}-k)t]\phi(\vec{k})\ , \tag{B3a}$$

$$=-ig(t)\ , \tag{B3b}$$

where γ_a and γ'_a are the spontaneous decay rates from level a to c and b, respectively, and Eq. (B3b) defines the pulse-shape function $g(t)$.[16,17] From here on we assume that γ'_a is negligibly small.

From Eq. (B3b) we then have

$$\alpha^a(t)=-i\exp(-\gamma_a t)\int_0^t dt_1\exp(\gamma_a t_1)g(t_1)\ , \tag{B4}$$

and from Eq. (B2) we have

$$\alpha^c_{\vec{k}_1}(t)=(-i)^2M_{\vec{k}_1}\int_0^t dt_1\exp[-\gamma_a-i(\Delta_{ac}-k_1)]t_1\times\int_0^{t_1}dt_2\exp(\gamma_a t_2)g(t_2)\ . \tag{B5}$$

The time-delayed photocounts $N(\Delta,\theta)$ can be obtained by substituting Eq. (B4) or (B5) into Eq. (2.14). $N(\Delta,\theta)$ depends on the pulse shape through the function $g(t)$.

For an exponentially decreasing pulse, the pulse-shape function $g(t)$ takes the form

$$g(t)=g_e\exp[(-\gamma_b-i\Delta)t]\ , \tag{B6}$$

where g_e is a constant, $\Delta=k_0-\Delta_{ab}$, k_0 is the central frequency of the pulse, and γ_b is the decay constant of the pulse. Substituting Eq. (B6) into Eq. (B4) or (B5), and using Eq. (2.14), we obtain Eq. (2.7) for the time-delayed count $N(\Delta,\theta)$.

For a square pulse of duration t_0, we have

$$g(t)=\begin{cases}g_s\exp(-i\Delta t), & 0\le t\le t_0\\ 0, & t>t_0\end{cases} \tag{B7}$$

where g_s is a constant, k_0 is again the central frequency of the pulse, and $\Delta=k_0-\Delta_{ab}$. Substituting Eq. (B7) into Eqs. (B4) and (B5), we obtain

$$\alpha^a(t)=\begin{cases} -ig_s \exp(-\gamma_a t)\int_0^t dt_1 \exp[(\gamma_a - i\Delta)t_1], \quad 0\le t\le t_0 & \text{(B8a)} \\ -ig_s \exp(-\gamma_a t)\int_0^{t_0} dt_1 \exp[(\gamma_a - i\Delta)t_1], \quad t>t_0 & \text{(B8b)} \end{cases}$$

and, for $t>t_0$,

$$\alpha^c_{\vec{k}_1}(t)=(-i)^2 g_s M_{\vec{k}_1}\left[\int_0^{t_0} dt_1 \exp[-\gamma_a - i(\Delta_{ac}-k_1)]t \int_0^{t_1} dt_2 \exp[(\gamma_a - i\Delta)t_2] + \int_{t_0}^{t} dt_1 \exp[-\gamma_a - i(\Delta_{ac}-k_1)]t_1 \int_0^{t_0} dt_2 \exp[(\gamma_a - i\Delta)t_2]\right]. \quad \text{(B9)}$$

Substituting Eq. (B8) or (B9) into Eq. (2.14), we obtain Eqs. (2.15) for the time-delayed photocounts.

[1]For a recent review see, for instance, *Laser Spectroscopy IV*, edited by H. Walther and K. W. Rothe (Springer, Berlin, Heidelberg, and New York, 1979).

[2]P. Meystre, M. O. Scully, and H. Walther, Opt. Commun. 33, 153 (1980).

[3]See, for example, M. Sargent III, M. O. Scully, and W. E. Lamb, Jr., *Laser Physics* (Addison-Wesley, Reading, Mass., 1974).

[4]P. L. Knight and P. E. Coleman, J. Phys. B 13, 4345 (1980).

[5]H. Metcalf and W. Phillips, Opt. Lett. 5, 540 (1980).

[6]F. J. Lynch, R. E. Holland, and M. Hamermesh, Phys. Rev. 120, 513 (1960).

[7]C. S. Wu, Y. K. Lee, N. Beczer-Koller, and P. Simms, Phys. Rev. Lett. 5, 432 (1960).

[8]G. Copley, B. P. Kibble, and G. W. Series, J. Phys. B 1, 724 (1968).

[9]P. Schenck, R. C. Hilborn, and H. Metcalf, Phys. Rev. Lett. 31, 189 (1973).

[10]H. Figger and H. Walther, Z. Phys. 267, 1 (1974).

[11]J. S. Deech, P. Hannaford, and G. W. Series, J. Phys. B 7, 1131 (1974).

[12]V. W. Hughes, in *Quantum Electronics*, edited by C. Townes (Columbia University Press, New York, 1960), p. 582.

[13]C. W. Fabjan and F. M. Pipkin, Phys. Rev. A 6, 556 (1972).

[14]S. R. Lundeen and F. M. Pipkin, Phys. Rev. Lett. 34, 1368 (1975).

[15]The difficulties associated with the definition of a time-dependent spectrum are given in J. H. Eberly and K. Wodkievicz, J. Opt. Soc. Am. 67, 1252 (1977).

[16]H. W. Lee, Ph.D. thesis, University of Pittsburgh, 1977 (unpublished).

[17]H. W. Lee and P. Stehle, J. Phys. B 11, 3015 (1978).